Journal of Inflammation Research

Dovepress
Taylor & Francis Group

Open Access Full Text Article

ORIGINAL RESEARCH

The Improvement of Intestinal Mucosal Epithelial Barrier Integrity by 1,3,4-Oxadiazole Derivatives of Pyrrolo[3,4-*d*]pyridazinone in Rat Experimental Colitis

Marta Szandruk-Bender[1], Benita Wiatrak[1], Anna Merwid-Ląd[1], Stanisław Dzimira[2], Adam Szeląg[1], Jan M Magdalan[1], Łukasz Szczukowski[3], Piotr Świątek[3], Anna Duda-Madej[4], Tomasz Gębarowski[5], Beata Nowak[1]

[1]Department of Pharmacology, Faculty of Medicine, Wroclaw Medical University, Wrocław, Poland; [2]Department of Pathology, Wroclaw University of Environmental and Life Sciences, Wrocław, Poland; [3]Department of Medicinal Chemistry, Faculty of Pharmacy, Wroclaw Medical University, Wrocław, Poland; [4]Department of Microbiology, Faculty of Medicine, Wroclaw Medical University, Wrocław, Poland; [5]Department of Biostructure and Animal Physiology, Wrocław University of Environmental and Life Sciences, Wrocław, Poland

Correspondence: Marta Szandruk-Bender, Department of Pharmacology, Wroclaw Medical University, Mikulicza-Radeckiego 2, Wrocław, 50-345, Poland, Email marta.szandruk@umw.edu.pl; Beata Nowak, Department of Pharmacology, Wroclaw Medical University, Mikulicza-Radeckiego 2, Wrocław, 50-345, Poland, Email beata.nowak@umw.edu.pl

Background and Purpose: The intestinal mucosal barrier is a complex structure that separates the internal and lumen environments. An impaired intestinal barrier may lead to excessive mucosal immune system activation and further to intestinal diseases, including inflammatory bowel disease (IBD). Therefore, improving the integrity of the intestinal barrier may be a therapeutic approach to prevent or treat IBD. In this study, we aimed to elucidate the effects of the new 1,3,4-oxadiazole derivatives of pyrrolo[3,4-*d*] pyridazinone, compounds **7b, 10b**, and **13b**, in intestinal epithelial damage.

Methods: In this study, we used biobank colon and feces samples collected during our previous original experiment, in which we induced colitis in rats by trinitrobenzenesulfonic acid (TNBS) administration. We assessed the expression of tight junction (TJ) proteins, ie, claudin 1 (CLDN1), occludin (OCLN), zonula occludens 1 (ZO1), and mucus layers proteins, ie, mucin 2 (Muc2) and trefoil factor 3 (TFF3), and the goblet cells and mucus content in colon tissues. We also assessed matrix metalloproteinase 9 (MMP9) and MAP kinases (MAPKs) levels in colon tissues and the level of α1-antitrypsin (α1-AT) in feces samples.

Results: We found that compounds **7b** and **13b** at a dose of 20 mg/kg prevented TNBS-induced loss of goblet cells and mucus layer with normalizing Muc2 and TFF3 expression. Both these compounds prevented TNBS-induced loss of the TJ proteins and normalized the fecal α1-AT level. Compounds **7b** and **13b** (20 mg/kg) counteracted the TNBS-induced increase of MMP9 concentration and MAPK activation.

Conclusion: New pyrrolo[3,4-*d*]pyridazinone derivatives normalized the colonic expression of TJ and mucus layer proteins and prevented goblet cells and mucus depletion in rats with experimental colitis, exerting a beneficial effect on mucosal epithelial barrier integrity. They protect against intestinal barrier dysfunction, and the potential mechanism may involve the inhibition of MAPKs and MMP9 activation.

Keywords: inflammatory bowel disease, tight junctions, mucus layer, goblet cell, trinitrobenzenesulfonic acid

Introduction

An enormous load of both essential and harmful molecules inside the intestinal lumen makes the selectively permeable intestinal mucosal epithelial barrier (so-called intestinal barrier) indispensable for maintaining intestinal homeostasis.[1,2] The intestinal barrier is a physical barrier consisting of the epithelial layer and the mucus layer, additionally strengthened by biochemical and immunological components.[3] A single sheet of columnar epithelial cells interspersed with

Received: 3 April 2025
Accepted: 26 June 2025
Published: 22 July 2025

functionally specialized epithelial cells, including goblet cells, forms an epithelial layer whose adjacent cells are connected by tight junctions.[4] Tight junctions are composed of a complex network of proteins, including transmembrane proteins such as claudins (CLDN) and occludin (OCLN) interacting with cytoplasmic proteins such as zonula occludens (ZO) proteins which connect to the actin cytoskeleton.[5,6] The epithelial layer is coated with a dense layer of mucus constitutively synthesized and secreted by the goblet cells. Intestinal mucus forms a hydrated, highly organized network of proteins, including mucins and trefoil peptides, especially mucin 2 (Muc2) and trefoil factor 3 (TFF3).[4,7]

In healthy individuals, the intact intestinal barrier allows water and nutrient absorption, on the one hand, and shields the body interior from the passage of luminal antigens and microorganisms, on the other hand.[6] Acting together, the tight junctions and mucus layer are believed to prevent excessive permeation of the luminal antigens across the epithelium, and their contact with the underlying lamina propria immune system, thus protecting the intestines from unwanted immune reactions.[2,8]

However, the intestinal mucosal barrier is a highly dynamic structure. Many factors may interfere with the integrity of the tight junctions and mucus layer, thereby leading to increased intestinal permeability resulting in penetration of luminal constituents into the lamina propria immune system and excessive antigenic stimulation of nonspecific and specific immune response.[1] Among factors that can disrupt the intestinal mucosal barrier and thus alter intestinal permeability are matrix metalloproteinase 9 (MMP9) and mitogen-activated protein kinases (MAPKs), including extracellular signal-regulated kinase-1/2 (ERK1/2), c-Jun N-terminal kinase (JNK), and p38 kinase.[9,10]

The impaired intestinal barrier can lead to subclinical but chronic immune system activation that might, in turn, contribute to the pathogenesis of intestinal diseases, including inflammatory bowel disease (IBD).[8] Moreover, recently, increasing evidence indicates a possible correlation of impaired intestinal barrier with several extraintestinal disorders, such as metabolic syndrome, obesity, non-alcoholic fatty liver disease, diabetes, inflammatory joint diseases, and also neurodegenerative disorders, such as Parkinson's disease or Alzheimer's disease.[11] Thus, improving the integrity and function of the intestinal mucosal barrier, especially the tight junctions and the mucus layer, may represent a therapeutic approach to prevent or treat diseases driven by luminal antigens, including IBD.[5,6]

Intestinal barrier dysfunction has emerged as a critical factor in the pathogenesis of IBD, including both Crohn's disease (CD) and ulcerative colitis (UC). In IBD, intestinal barrier integrity is compromised at various levels.[6] Damage to epithelial cells contributes to impaired barrier function and involves both secretory cells, mainly goblet cells, as well as absorptive epithelial cells. These cells undergo functional changes, producing reduced amounts of antimicrobial peptides and other soluble factors that play a crucial role in maintaining intestinal barrier integrity. Goblet cell dysfunction and reduced production of Muc2 compromise the protective mucus layer, particularly in UC, facilitating direct contact between luminal microbes and epithelial cells.[5] Paneth cell dysfunction, often observed in CD (especially in patients with ATG16L1 or NOD2 mutations), results in defective secretion of antimicrobial peptides, weakening another critical arm of mucosal defense.[6] In IBD patients, the intestinal epithelial barrier is also disrupted due to structural and functional alterations in tight junctions, leading to increased paracellular permeability. IBD patients present a decrease in sealing claudins, primarily claudin-1, -3, -5, -8, and occludin, and an upregulation of the pore-forming claudin-2, which is induced by TNF-α and facilitates increased paracellular transport of cations and water. A hallmark of IBD is a reduced level of ZO1. Under physiological conditions, ZO1 is involved in the regulation of fluid, macromolecule, and leukocyte transport between the bloodstream and the intestinal lumen. It also plays a role in protecting the proximal intestine from microbial colonization, contributing to innate immunity.[5,6] This disruption leads to enhanced paracellular ion and solute flux and promotes the translocation of bacteria and their components, such as lipopolysaccharide, flagellin, and muramyl dipeptide, into the lamina propria. There, they are recognized by innate immune receptors, including Toll-like receptors (TLRs) and nucleotide-binding oligomerization domain-like receptors (NODs), triggering and amplifying an abnormal immune response. This response is marked by excessive production of proinflammatory cytokines, including TNF-α, IL-1β, IL-6, IL-17, and IL-23, which further compromise epithelial integrity, establishing a vicious cycle of inflammation and tissue damage.[6,7] Genetic studies have revealed that several IBD-associated susceptibility genes, such as NOD2, MUC2, ATG16L1, CDH1, and IRGM, are directly involved in epithelial function, autophagy, and barrier integrity, suggesting that barrier dysfunction is not merely a consequence of inflammation but rather a driver of disease. Studies in first-degree relatives of IBD patients have shown subclinical defects in intestinal permeability and TJ protein expression,

indicating that barrier abnormalities may precede the onset of clinical disease.[2,5] The integrity of the intestinal barrier also relies on a finely regulated immune balance, especially between Th17 and Treg cell lineages. In healthy conditions, Th17 cells secrete IL-17 and IL-22 cytokines, which contribute to host defense and epithelial regeneration, while Treg cells limit excessive immune activation and support epithelial repair by secreting IL-10. However, in IBD, the Th17/Treg balance is disrupted.[12,13] Excessive Th17 activity promotes inflammation and disrupts TJ protein expression by IL-17 and IL-22, increasing intestinal permeability. Th17 activity predominating over Treg can alter goblet cell function and Muc2 synthesis, thinning of the mucus layer.[6]

With the above in mind, therapeutic strategies aimed at restoring barrier integrity offer a promising approach to treat this devastating disease, IBD. Targeting epithelial repair, tight junction modulation, and mucus layer reinforcement may help reduce microbial translocation and secondary immune activation.[5] In medicinal chemistry, a commonly adopted strategy for developing new bioactive compounds is to merge a scaffold with known biological activity with pharmacophoric groups that can enhance efficacy while minimizing toxicity. The compounds studied here are structurally based on a pyridazinone core, recognized for its anti-inflammatory properties, combined with variously substituted five-membered oxadiazole rings. The introduction of the oxadiazole moiety not only reduces the likelihood of adverse effects but also increases molecular lipophilicity, potentially improving membrane permeability and target site accessibility. Moreover, the oxadiazole ring has been linked to greater selectivity toward cyclooxygenase 2 (COX2) and the ability to modulate the STAT3 signaling pathway, which plays a key role in the differentiation of Th17 cells.[12–15] We have previously shown that the new pyrrolo[3,4-*d*]pyridazinone derivatives, ie, 6-butyl-3,5,7-trimethyl-1-[[3-[(4-phenylpiperazin-1-yl)methyl]-2-thioxo-1,3,4-oxadiazol-5-yl]methoxy]pyrrolo[3,4-*d*]pyridazin-4-one and 6-butyl-3,5,7-trimethyl-1-[[3-[[4-(4-nitrophenyl)piperazin-1-yl]methyl]-2-thioxo-1,3,4-oxadiazol-2-yl]methoxy]pyrrolo[3,4 d]pyridazin-4-one and 6-butyl-1-[[3-[[4-(4-chlorophenyl)-4-hydroxy-1-piperidyl]methyl]-2-thioxo-1,3,4-oxadiazol-5-yl]methoxy]-3,5,7-trimethyl-pyrrolo[3,4-*d*]pyridazin-4-one, hereafter called the compounds **7b, 10b**, and **13b**, respectively, strongly inhibit COX activity with a better affinity for the COX2 isoenzyme, normalize the level of PGE_2 and reduce the influx of inflammatory cells to the site of the ongoing inflammation.[12,14,15] Since COX2 and PGE_2 play an important role in the regulation of the Th17/Treg axis, we decided to check whether these new compounds affect the Th17/Treg axis. In our earlier paper, we revealed that they do. The studied compounds targeted the Th17 developmental pathway by reducing the expression of RORγt, STAT3, and IL-23, as well as the Treg developmental pathway by enhancing the expression of Foxp3.[13]

The current study was designed to further elucidate the mechanisms involved in the protective effect of the new pyrrolo[3,4-*d*]pyridazinone derivatives in the course of experimental colitis. Considering that the studied compounds influence the Th17/Treg axis' components and the Th17/Treg imbalance contributes to epithelial damage and barrier dysfunction in IBD, in the current study, we aimed to investigate, whether the protective effect of the new pyrrolo[3,4-*d*]pyridazinone derivatives involved the alleviation of intestinal barrier impairment by increasing the expression of TJ proteins and mucus layer proteins. Additionally, to further assess the mechanisms by which these new compounds protected the intestinal mucosal barrier, we examined the levels of MMP9 and total and phosphorylated MAP kinases (ERK1/2, JNK, p38).

Materials and Methods

This follow-up study was conducted on the colon tissue and feces samples collected during our earlier original experiment.[13] The design of the original experiment and methods used for the purpose of the present study are described below.

Studied Compounds

New 1,3,4-oxadiazole derivatives of pyrrolo[3,4-*d*]pyridazinone, named **7b, 10b**, and **13b**, were obtained from the Department of Medicinal Chemistry, Wroclaw Medical University, Poland. The project of the synthesis of the studied compounds has been described earlier.[14] The structure and purity of the studied compounds were confirmed by various spectroscopic and analytical methods. Based on NMR and ESI-MS spectra, the purity of the studied compounds was > 95%.

Animals

The current study was performed on the colon tissue and feces samples taken during our previous experiment approved by the Local Ethics Committee for Animal Experiments in Wrocław at Hirszfeld Institute of Immunology and Experimental Therapy of the Polish Academy of Sciences (Wrocław, Poland, Resolution No. 005/2020 of 15 January 2020) and described in detail in the previously published paper.[13] The experiment was carried out on Wistar male rats (Animal Research Center at Wroclaw Medical University, Wrocław, Poland) weighing 210–260 g, kept two per cage with enrichments under standard and controlled laboratory conditions, ie, 12-hour light/12-hour dark cycle, 55–60% humidity, 21–24°C temperature, free water access, and free standard pelleted animal feed access except for one deprivation procedure.

The Design of in vivo Experiment, Colitis Induction, and Samples Collection

The rats were randomly allocated to 8 following groups of 10 animals each: one group received vehicle (0.5% carboxymethylcellulose solution) intragastrically (i.g.) and once normal saline rectally (p.r.) – control group; one group received vehicle i.g. and once trinitrobenzenesulfonic acid (TNBS) solution p.r. – colitis (TNBS) group; and 6 groups received i.g. compound **7b** or **10b** or **13b** at the doses of 10 or 20 mg/kg and once TNBS solution p.r. – **7b**-10, **7b**-20, **10b**-10, **10b**-20, **13b**-10, **13b**-20 groups, respectively. The studied substances' doses were selected based on earlier studies.[12,15]

During the 16-day pretreatment, vehicle alone or studied compounds were administered in a volume of 4 mL/kg once daily via a gastric tube (FST, Foster City, CA, USA). On the 15th day of the experiment, after 12 hours of food deprivation, the rats were anesthetized by inhalation of isoflurane (4–5% for induction, 2–3% for maintenance, CP-Pharma, Burgdorf, Germany), placed on their right side, and experimental colitis was induced according to the procedure originally described by Morris et al.[16] The ethanol solution (50%, v/v) of TNBS (50 mg/kg, Sigma-Aldrich, Steinheim, Germany) was given by a flexible catheter into the colon through the rectum with the tip placed 8 cm proximal to the anus, except the control group in which rats were instilled with normal saline given by the same route and in equivalent volume. Then, rats were kept in the Trendelenburg position for 5 min to avoid leakage of the instilled solution.

On the 17th day of the experiment (48 h after colitis induction), the feces samples were collected, frozen, and stored at −80°C for ELISA assay, and then rats were sacrificed by intramuscular injection of medetomidine at a dose of 0.5 mg/kg (Orion Pharma, Warszawa, Poland) followed by intraperitoneal injection of pentobarbital at a dose of 200 mg/kg (Biowet, Puławy, Poland). Afterward, the distal 8 cm long colon sections were taken, opened longitudinally, cleaned, and portioned for different analyses into three parts. The first part was fixed in 4% buffered formalin, processed by routine techniques, and stained with alcian blue for histological assessment. The second part was frozen and stored at −80 °C for ELISA and multiplex assays. The third part of the colon samples was snap-frozen, embedded in an O.C.T. compound, and sectioned with a cryostat (Leica CM1850, Leica Biosystems, Nussloch, Germany) for immunohistochemistry studies.

Microscopic Evaluation of the Colon Tissues

The formalin-fixed colon tissue specimens were embedded in paraffin, sectioned into 4-μm thick slices, mounted on the glass slides, deparaffinized, rehydrated, and stained with Alcian blue to evaluate the goblet cells and mucus content. The evaluation was performed in a blinded way by an experienced pathologist. Analysis and microphotographs of colon tissue samples were taken under light microscopy with an Olympus BX53 microscope equipped with a UC90 camera with the software Olympus cellSense Standard ver. 1.0 (Olympus Soft Imaging Solutions GmbH, Germany) at 100× magnification. Alcian blue-stained specimens were assessed on a 0–6 modified scale, which considers goblet cells and mucus content based on the scale described by Zhang et al.[17] The scoring scale was as follows: 0 – normal quantity and distribution of goblet cells and mucus throughout the colon, 1 – mild goblet cell and mucus disorganization, 2 – increased goblet cell and mucus accumulation at the luminal surface, 3 – hyperplastic goblet cells, 4 – loss of goblet cells and less densely packed distribution of mucin, 5 – extensive goblet cell depletion and loss of crypt architecture, 6 – complete goblet cell depletion and mucus layer decline.

Immunohistochemical Evaluation of Muc2 and TFF3 Expression in the Colon Tissues

The levels of Muc2 and TFF3 were detected immunohistochemically in the freshly collected, snap-frozen colon tissue samples without fixation in formalin, accordingly to standard procedures. The 4-μm thick colon tissue sections were prepared in a cryostat. The cryosections were fixed with 100% cold (−20°C) methyl alcohol (PolAura, Olsztyn, Poland) for 5 min. The tissue sections were then washed three times with 0.1% Tween 20 in PBS (PBST, PolAura, Olsztyn, Poland) for 5 min. In the next step, the cell membrane was permeabilized with 0.1% Triton X-100 solution in PBS for 10 min at room temperature. Then, the incubation with a solution of 1% BSA and 10% NGS (PolAura, Olsztyn, Poland) in PBST for 30 min was carried out to block unspecific antibody binding. Antibodies diluted in the appropriate proportions in 1% BSA in PBST were added in the next step: anti-Muc2 (Abcam, Cambridge, UK) was dissolved to a final concentration of 5 μg/mL and anti-TFF3 (Novus Biologicals, Abingdon, UK) at a ratio of 1:100, and incubated with colon tissue sections overnight in the dark at room temperature. The next day, slides were washed in PBS three times for 5 min and incubated with a secondary antibody Goat Anti-Rabbit IgG H&L conjugated with Alexa Fluor 488 dye (Abcam, Cambridge, UK) prepared in 1% BSA and 10% NGS in PBST for 1 hour in the dark at room temperature. Finally, counterstaining with DAPI (Sigma Aldrich, Steinheim, Germany) was performed at room temperature. Rinsing in PBS for 5 min was repeated three times. Vectashield mounting medium (Vector Laboratories, Burlingame, CA, USA) was then applied to prevent discoloration, and the slides were secured with coverslips. The whole colon tissue sections were assessed under a fluorescence microscope EVOS FL Auto Imaging System (Thermo Fisher Scientific, Waltham, MA, USA), which enables a large area of the tissue sample to be scanned and obtain multiple images to build a tiled and stitched image ultimately. Then, with proprietary software, the expression intensity of the examined parameters was quantified. The color intensity for individual cells was analyzed (detected via counterstaining), and only on this basis were the mean intensities for individual images calculated. Additionally, tissue areas were delineated, which made it possible to calculate the number of cells per % of tissue.

ELISA Determination of CLDN1, OCLN, ZO1, and MMP9 Levels in the Colon Tissues

The colon tissues were homogenized in 1×PBS using Homogenizer PRO250 (PRO Scientific Inc., Oxford, CT, USA) on ice. After two freeze-thaw cycles, the homogenates were centrifuged (9000 rpm, 4°C, 5 min) using an MPW-350R laboratory centrifuge (MPW Med. Instruments, Warszawa, Poland), and supernatants were collected, aliquoted, and stored at −80°C until the analyses. The concentration of tight junction proteins (CLDN1, OCLN, ZO1), and protease MMP9 was quantified in the obtained supernatants by ELISA assay using Rat CLDN1 ELISA Kit, Rat OCLN ELISA Kit, Rat ZO1 ELISA Kit, and Rat MMP9 ELISA Kit (ELK Biotechnology Co., Ltd, Wuhan, China). All ELISAs were made in accordance with the manufacturers' instructions. The concentration of CLDN1 was given in pg/mL and the levels of OCLN, ZO1, and MMP9 were expressed in ng/mL.

ELISA Determination of the Fecal α1-AT Level

Feces were homogenized after adding 1×PBS using a Homogenizer UP100H (Hielscher Ultrasonics GmbH, Teltow, Germany). The supernatants were collected after centrifuging at 3000 rpm and 4°C for 20 min. The level of α1-antitrypsin in feces samples was quantified using the Rat α1-Antitrypsin ELISA Kit (SunLong Biotech Co., LTD, Hangzhou, Zhejiang, China), as described by the manufacturer, and results were given in ng/mL.

Multiplex Determination of Total and Phosphorylated ERK1/2, JNK, and p38 Levels in the Colon Tissues

The colon tissues were homogenized in cold Milliplex Lysis Buffer with Protease Inhibitor Cocktail (Merck Millipore, Darmstadt, Germany) using Homogenizer PRO250 (PRO Scientific Inc., Oxford, CT, USA) on ice. The homogenates were centrifuged (9000 rpm, 4°C, 5 min) using an MPW-350R laboratory centrifuge (MPW Med. Instruments, Warszawa, Poland), and supernatants were collected, aliquoted, and stored at −80°C until the analyses. The levels of total and phosphorylated ERK1/2, JNK, p38 were assessed in the obtained supernatants using multiplexed fluorescence microsphere immunoassays with Milliplex Kits: the Milliplex Multi-Pathway Signaling Total Magnetic Bead Multiplex

Kit and Milliplex Multi-Pathway Signaling Magnetic Bead Multiplex Kit-Phosphoprotein (Merck Millipore, Darmstadt, Germany) according to the manufacturer's instructions. The analysis and quantification were carried out using Magpix Instrument (Merck Millipore, Darmstadt, Germany) with the xPONENT 4.2 Software. Results were reported in median fluorescence intensity (MFI) and normalized to the total protein concentration. The total protein concentration in supernatants was measured in a certified laboratory using Architect c4000 equipment and commercial Total Protein Architect Abbott Kit (Abbott, Wiesbaden, Germany) following the manufacturer's instructions. The ratio of the phosphoproteins relative to the corresponding total proteins was also calculated (phosphorylated/total ratio).

Statistical Analysis

The quality of the obtained data was assessed by analyzing the normal distribution (Shapiro–Wilk test) and the equality of variance (Brown-Forsythe test). Based on the results, parametric tests were used for statistical analysis. Thus, the one-way analysis of variance (ANOVA) was performed to assess the significance of differences between the study groups, followed by Tukey's post hoc test. Data in the graphs and tables are presented as mean ± standard deviation (SD). The multiple-criteria decision analysis (MCDA) in the weighted sum model was carried out to summarize the results achieved in all assays performed and compare the pharmacological activity of the studied compounds. The weights were assumed equal for all assays performed. The results of each assay were additionally normalized before the analysis so that the maximal effect obtained in one assay should have the same significance for the final result as the maximal effect obtained in other assays. Statistical analysis was performed in GraphPad Prism version 8.0 (GraphPad Software, San Diego, CA, USA) and Tibco Statistica version 13.3 (StatSoft, Kraków, Poland). The significance level was set at $p < 0.05$.

Results

Pyrrolo[3,4-*d*]pyridazinone Derivatives Prevented Goblet Cells and Mucus Depletion in Rats with TNBS-Induced Colitis

To evaluate whether the studied compounds prevent the TNBS-induced changes in goblet cells and mucus content, histopathological analysis of Alcian blue-stained colon tissue specimens was performed. Figure 1b shows the scoring of Alcian blue-stained colon tissue samples. After the development of TNBS-induced colitis, loss of goblet cells, their irregular structure, and a notable decrease in mucus content were observed compared to the control rats ($p < 0.001$), in which numerous mucus-filled goblet cells and normal distribution of mucus throughout the colon were visible (Figure 1aA and aE). In the colon tissues of TNBS-subjected rats, goblet cells were damaged in the area of mucosal injury, and mucus was located extracellularly in the damaged and swollen submucosa. There were no goblet cells in the center of the ulcer, a small number around the periphery of the ulcer, and a normal number only in the intact mucosa (Figure 1aE). Upon pretreatment with compound **7b** at both doses tested (10 or 20 mg/kg), the TNBS-caused destruction was reverted. The increased number of goblet cells, increased amount of mucus, and closely packed crypt architecture were noticed ($p < 0.01$, $p < 0.001$ vs TNBS group, respectively, and $p < 0.001$ vs control group in both comparisons, Figure 1aB and aF). Similarly, compound **13b** at a dose of 20 mg/kg, but not at a dose of 10 mg/kg, prevented the TNBS-induced changes in goblet cells and mucus content ($p < 0.01$ vs TNBS group and $p < 0.001$ vs control group, Figure 1aD and aH). Goblet cells in these three pretreated groups of rats were characterized by a regular structure and size, regular distribution in colonic crypts, and a large quantity of mucus (Figure 1aB, aF and aH). Neither low nor high dose compound **10b** exerted a significant effect on TNBS-caused alterations (p = NS vs TNBS group and $p < 0.001$ vs control group in both cases Figure 1aC and aG).

Pyrrolo[3,4-*d*]pyridazinone Derivatives Regulated the Colonic Expression of Muc2 and TFF3 in Rats with TNBS-Induced Colitis

To elucidate whether the studied compounds influence protein expressed within goblet cells, ie, Muc2 and TFF3, the immunohistochemical analysis was carried out, the results of which are presented in Figures 2 and 3. In the colon tissues assessed immunohistochemically, a significant decrease in the expression of Muc2 and TFF3 was observed in TNBS-subjected rats compared to healthy control rats ($p < 0.001$ and $p < 0.01$, respectively). Compounds **7b** and **13b** at a high dose, but not at a low dose counteracted the decreased expression of Muc2 and TFF3 compared to the TNBS group ($p <$

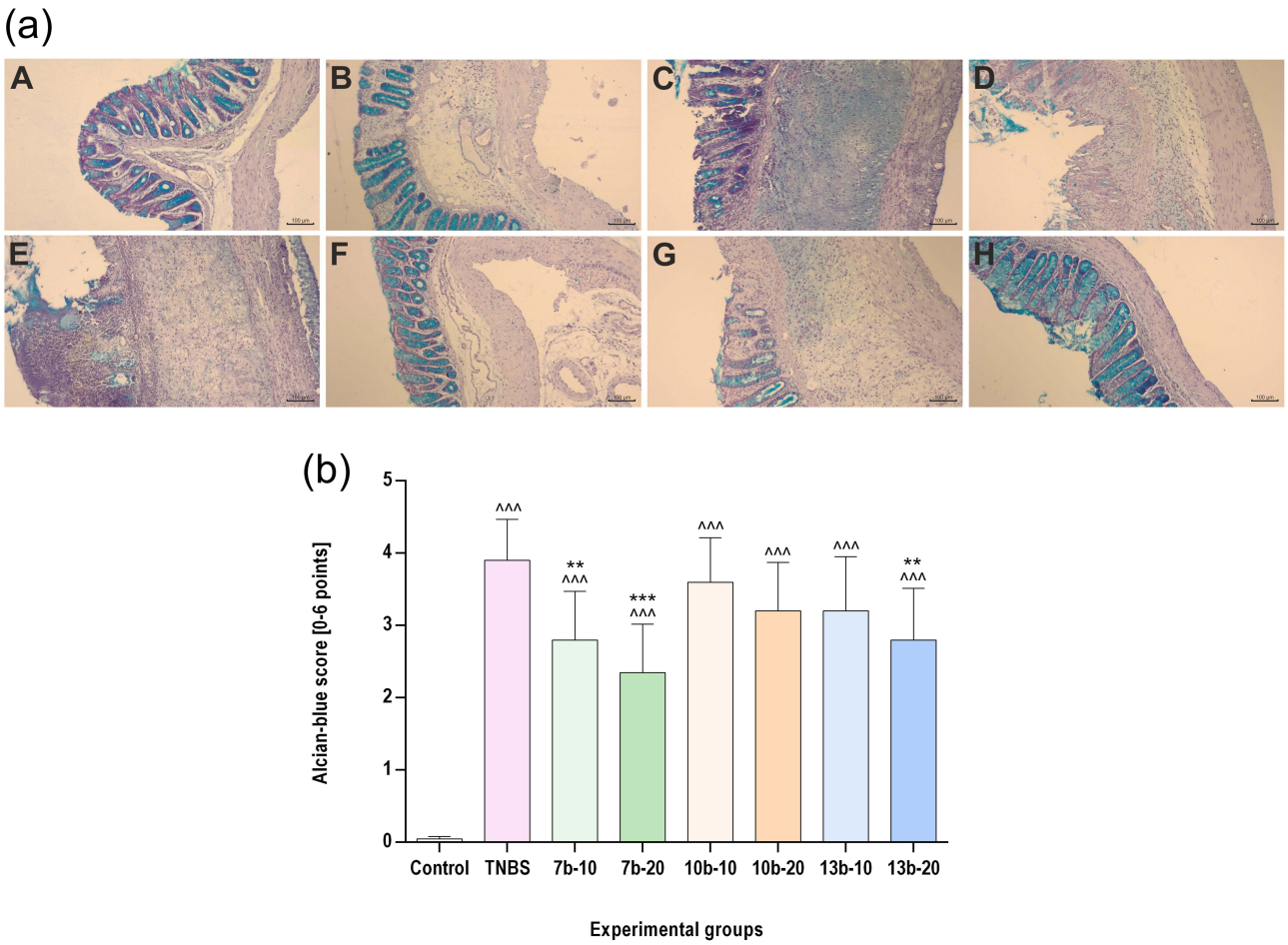

Figure 1 The influence of compounds **7b, 10b**, and **13b** on goblet cells and mucus content in the colon tissues in Alcian blue staining. (**a**) Microscopic images of the Alcian blue-stained colon tissues revealed that compound **7b** (10 and 20 mg/kg) and compound **13b** (20 mg/kg) prevented TNBS-induced loss of goblet cells and the mucus layer. Experimental groups: control group (A); group receiving 10 mg/kg compound **7b** and TNBS (B); group receiving 10 mg/kg compound **10b** and TNBS (C); group receiving 10 mg/kg compound **13b** and TNBS (D); group receiving only TNBS (E); group receiving 20 mg/kg compound **7b** and TNBS (F); group receiving 20 mg/kg compound **10b** and TNBS (G); group receiving 20 mg/kg compound **13b** and TNBS (H); magnification 100×. (**b**) Quantification of histopathological data. Experimental groups: control – control group; TNBS – group receiving only TNBS; **7b**-10, **7b**-20 – groups receiving, respectively, 10 or 20 mg/kg of studied compound **7b** and TNBS; **10b**-10, **10b**-20 – groups receiving, respectively, 10 or 20 mg/kg of studied compound **10b** and TNBS; **13b**-10, **13b**-20 – groups receiving, respectively, 10 or 20 mg/kg of studied compound **13b** and TNBS. Data are expressed as mean values ± SD; n = 10 for each group. Analyses were performed using the one-way ANOVA and Tukey's post hoc test. Differences ^^^$p < 0.001$ vs control group; **$p < 0.01$, ***$p < 0.001$ vs TNBS group were deemed statistically significant.

0.001 and $p < 0.01$ for Muc2 and TFF3, respectively). In turn, pretreatment with compound **10b** at either low or high doses caused no statistically significant increase in the expression of both parameters assessed compared to the TNBS group (p = NS in all comparisons). The effect of compound **7b** at a high dose on Muc2 and TFF3 expression was greater than that of compound **10b** at the corresponding dose (p <0.001 in both cases) and greater than that of compound **13b** at the corresponding dose ($p < 0.01$ and $p < 0.05$, respectively). Additionally, compound **7b** at a high dose was more effective than at a low dose on TFF3 expression ($p < 0.001$). Compound **13b** at a high dose acted more effectively than compound **10b** at the corresponding dose ($p < 0.05$) on TFF3 expression.

Pyrrolo[3,4-*d*]pyridazinone Derivatives Normalized the Colonic Expression of CLDN1, OCLN, ZO1, and MMP9 in Rats with TNBS-Induced Colitis

The levels of CLDN1, OCLN, and ZO1 were measured by ELISA assays to evaluate the tight junction integrity of the colon tissues (Figure 4A–C). The levels of CLDN1, OCLN, and ZO1 were significantly reduced in the TNBS group compared to the control group ($p < 0.001$ in all cases). Pretreatment with compound **7b** at a dose of 20 mg/kg, but not at a dose of 10 mg/kg, prevented the TNBS-induced decrease of all studied tight junction proteins and normalized their

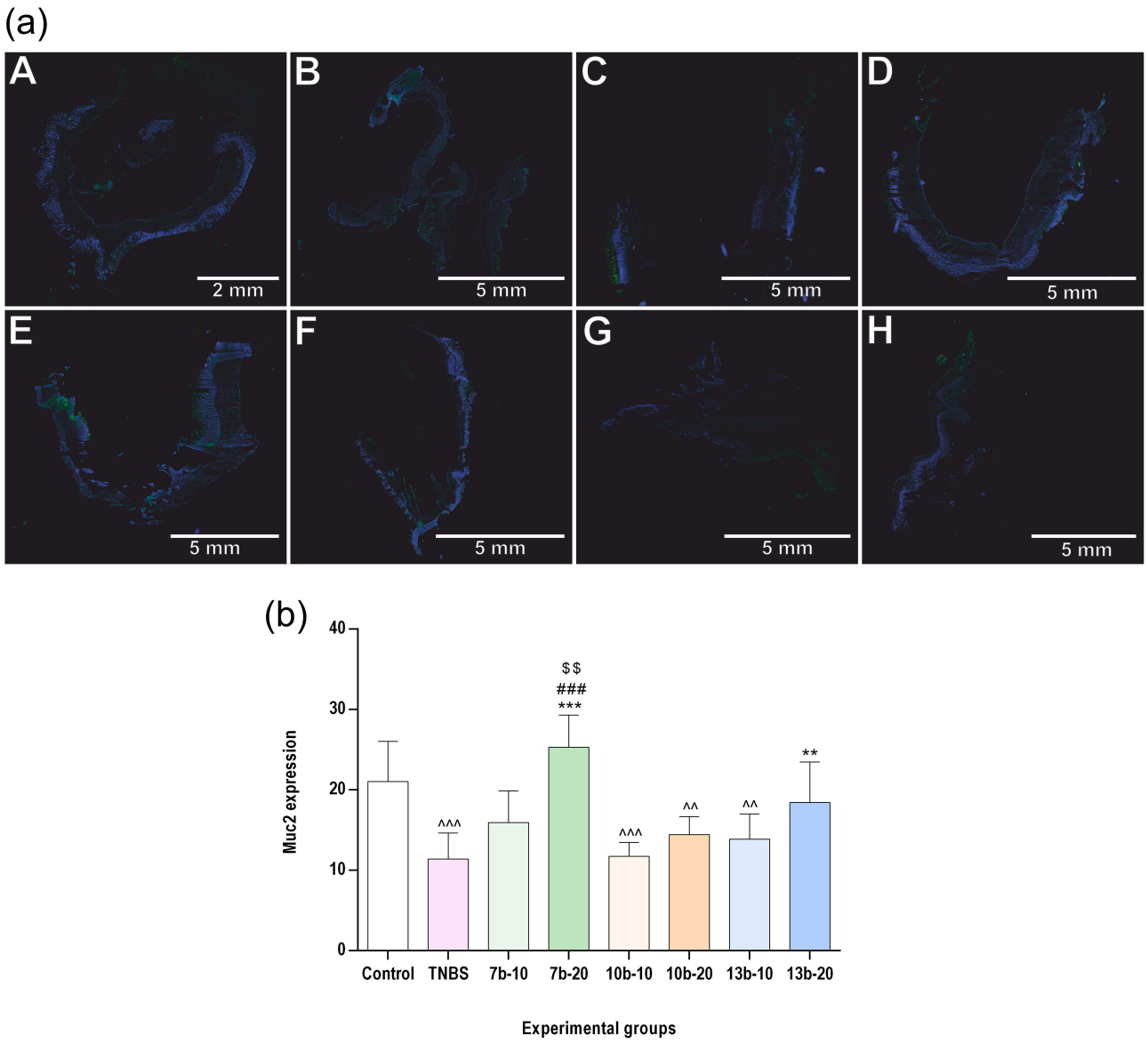

Figure 2 The influence of compounds **7b, 10b**, and **13b** on Muc2 expression in the colon tissues. (**a**) Microscopic images of cryosections of whole colon tissue samples after immunostaining with antibodies specific to Muc2 fluorescently detected showed that compounds **7b** and **13b** at a high dose counteracted TNBS-induced reduction in Muc2 expression; Anti-MUC2 antibody (ab90007, Abcam), rabbit polyclonal; Goat Anti-Rabbit IgG H&L Alexa Fluor 488 (ab150077, Abcam); Fluorophore: Alexa Fluor 488 (excitation: 495 nm, emission: 519 nm), detected in the green channel. Experimental groups: control group (A); group receiving 10 mg/kg compound **7b** and TNBS (B); group receiving 10 mg/kg compound **10b** and TNBS (C); group receiving 10 mg/kg compound **13b** and TNBS (D); group receiving only TNBS (E); group receiving 20 mg/kg compound **7b** and TNBS (F); group receiving 20 mg/kg compound **10b** and TNBS (G); group receiving 20 mg/kg compound **13b** and TNBS (H); magnification 4×. (**b**) Quantification of immunohistochemical data based on proprietary software. Experimental groups: control – control group; TNBS – group receiving only TNBS; **7b**-10, **7b**-20 – groups receiving, respectively, 10 or 20 mg/kg of studied compound **7b** and TNBS; **10b**-10, **10b**-20 – groups receiving, respectively, 10 or 20 mg/kg of studied compound **10b** and TNBS; **13b**-10, **13b**-20 – groups receiving, respectively, 10 or 20 mg/kg of studied compound **13b** and TNBS. Data are expressed as mean values ± SD; n = 10 for each group. Analyses were performed using the one-way ANOVA and Tukey's post hoc test. Differences $^{\wedge\wedge}p < 0.01$, $^{\wedge\wedge\wedge}p < 0.001$ vs control group; $^{**}p < 0.01$, $^{***}p < 0.001$ vs TNBS group; $^{\#\#\#}p < 0.001$ vs compound **10b** at the corresponding dose group; $^{\$\$}p < 0.01$ vs compound **13b** at the corresponding dose group were deemed statistically significant.

concentrations in the colon tissues compared to the colitis group ($p < 0.001$ in all cases). All studied tight junction protein concentrations in the high-dose compound **7b**-pretreated group were not different from the control group (p = NS in all comparisons). Compound **10b** at a high dose, but not at a low dose, prevented the decrease and normalized only CLDN1 and OCLN colonic levels ($p < 0.05$ vs TNBS group and p = NS vs control group in both cases). Compound **13b** only at a high dose protected from the decrease of all studied tight junction proteins and normalized their concentrations in the colon tissues compared to the colitis group ($p < 0.05$, $p < 0.01$, $p < 0.01$ respectively, and p = NS vs control group

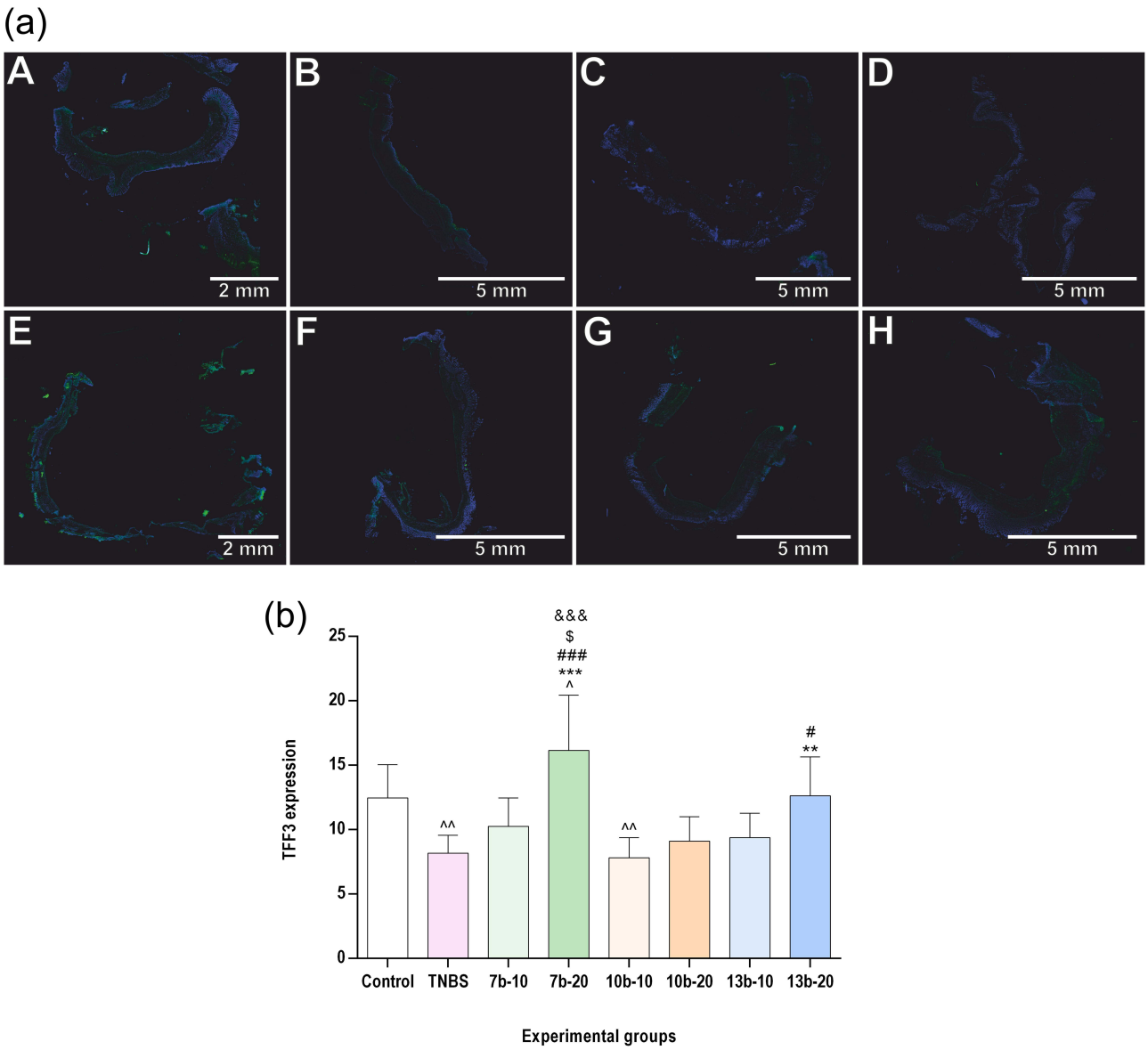

Figure 3 The influence of compounds **7b, 10b**, and **13b** on TFF3 expression in the colon tissues. (**a**) Microscopic images of cryosections of whole colon tissue samples after immunostaining with antibodies specific to TFF3 fluorescently detected showed that compounds **7b** and **13b** at a high dose counteracted TNBS-induced reduction in TFF3 expression; TFF3 Antibody (NBP1-76514, NovusBio), rabbit polyclonal; Goat Anti-Rabbit IgG H&L Alexa Fluor 488 (ab150077, Abcam); Fluorophore: Alexa Fluor 488 (excitation: 495 nm, emission: 519 nm), detected in the green channel. Experimental groups: control group (A); group receiving 10 mg/kg compound **7b** and TNBS (B); group receiving 10 mg/kg compound **10b** and TNBS (C); group receiving 10 mg/kg compound **13b** and TNBS (D); group receiving only TNBS (E); group receiving 20 mg/kg compound **7b** and TNBS (F); group receiving 20 mg/kg compound **10b** and TNBS (G); group receiving 20 mg/kg compound **13b** and TNBS (H); magnification 4×. (**b**) Quantification of immunohistochemical data based on proprietary software. Experimental groups: control – control group; TNBS – group receiving only TNBS; **7b**-10, **7b**-20 – groups receiving, respectively, 10 or 20 mg/kg of studied compound **7b** and TNBS; **10b**-10, **10b**-20 – groups receiving, respectively, 10 or 20 mg/kg of studied compound **10b** and TNBS; **13b**-10, **13b**-20 – groups receiving, respectively, 10 or 20 mg/kg of studied compound **13b** and TNBS. Data are expressed as mean values ± SD; n = 10 for each group. Analyses were performed using the one-way ANOVA and Tukey's post hoc test. Differences $^{\wedge}p < 0.05$, $^{\wedge\wedge}p < 0.01$ vs control group; $^{**}p < 0.01$, $^{***}p < 0.001$ vs TNBS group; $^{\#}p < 0.05$, $^{\#\#\#}p < 0.001$ vs compound **10b** at the corresponding dose group; $^{\$}p < 0.05$ vs compound **13b** at the corresponding dose group; $^{\&\&\&}p < 0.001$ vs compound **7b**-10 group were deemed statistically significant.

in all comparisons). Additionally, in the group pretreated with the higher dose of compound **7b** or compound **13b**, a significantly higher concentration of ZO1 was observed compared to the group of rats pretreated with compound **10b** at the corresponding dose ($p < 0.05$ in both cases).

The concentration of MMP9 was measured by ELISA assay to determine whether the intestinal barrier disruption is mediated by metalloproteinase 9 (MMP9) (Figure 4D). Compared to control rats, the content of MMP9 in the colon tissues

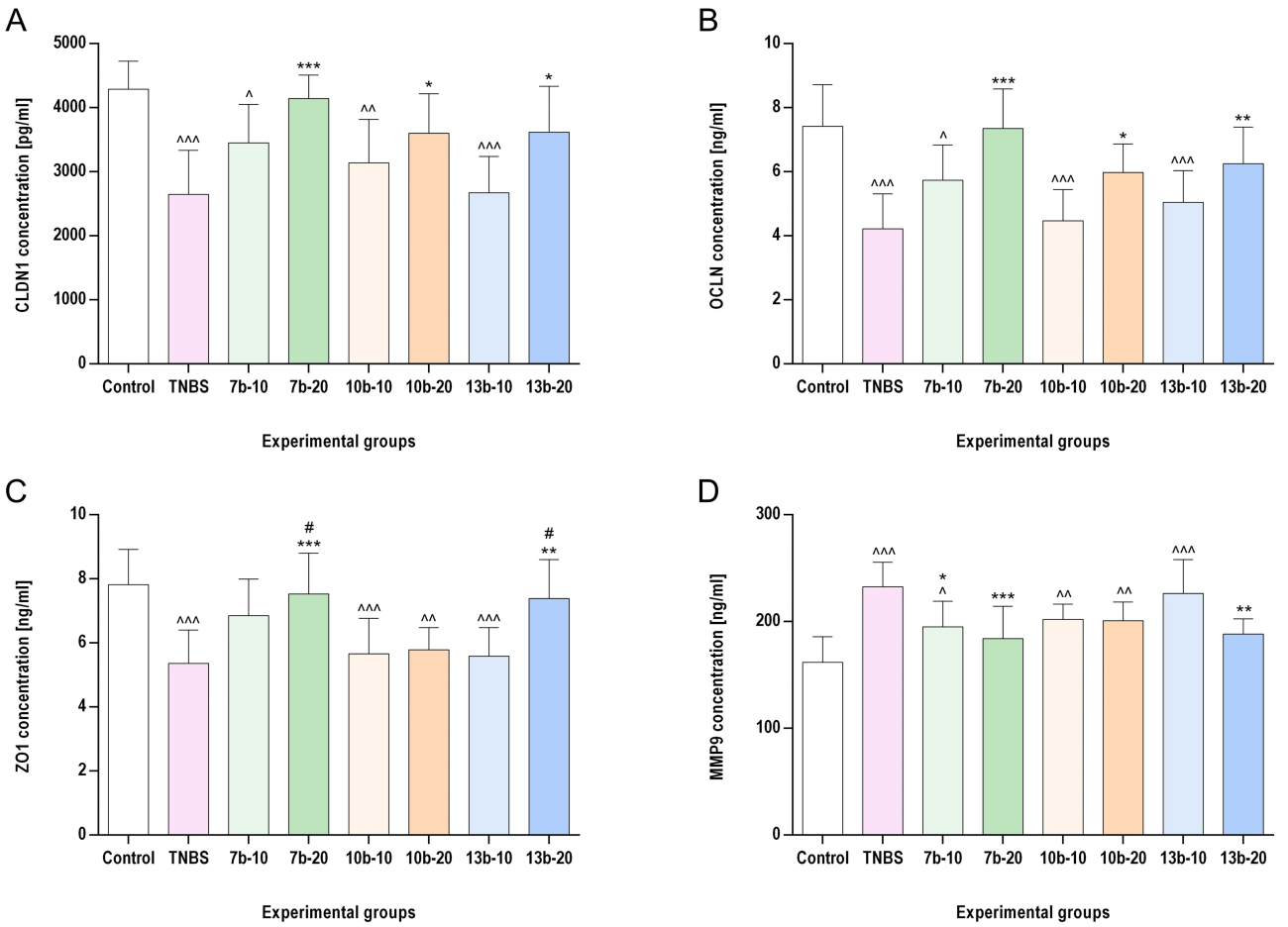

Figure 4 The influence of compounds **7b, 10b**, and **13b** on CLDN1 (**A**), OCLN (**B**), ZO1 (**C**), and MMP9 (**D**) concentrations in the colon tissues. Experimental groups: control – control group; TNBS – group receiving only TNBS; **7b**-10, **7b**-20 – groups receiving, respectively, 10 or 20 mg/kg of studied compound **7b** and TNBS; **10b**-10, **10b**-20 – groups receiving, respectively, 10 or 20 mg/kg of studied compound **10b** and TNBS; **13b**-10, **13b**-20 – groups receiving, respectively, 10 or 20 mg/kg of studied compound **13b** and TNBS. Data are expressed as mean values ± SD; n = 10 for each group. Analyses were performed using the one-way ANOVA and Tukey's post hoc test. Differences $^{\wedge}p < 0.05$, $^{\wedge\wedge}p < 0.01$, $^{\wedge\wedge\wedge}p < 0.001$ vs control group; $*p < 0.05$, $**p < 0.01$, $***p < 0.001$ vs TNBS group; $^{\#}p < 0.05$ vs compound **10b** at the corresponding dose group were deemed statistically significant.

was significantly increased in TNBS-subjected rats ($p < 0.001$). Administration of compound **7b** at both doses tested counteracted the increase of MMP9 concentration in comparison to the colitis group ($p < 0.05$, $p < 0.001$, respectively). Additionally, the high-dose compound **7b**-pretreated group did not differ from the control group (p = NS). After pretreatment with compound **13b** only at a high dose, the MMP9 level was lessened in comparison to TNBS-subjected rats ($p < 0.01$) and did not differ from that of control rats (p = NS). Neither low nor high dose compound **10b** exerted a significant effect on TNBS-caused alterations (p = NS vs TNBS group and $p < 0.01$ vs control group in both cases).

Pyrrolo[3,4-*d*]pyridazinone Derivatives Normalized the Fecal Concentration of α1-AT in Rats with TNBS-Induced Colitis

To assess intestinal permeability, fecal α1-antitrypsin was quantified by ELISA assay. These results are presented in Figure 5. The fecal level of α1-antitrypsin was markedly elevated in TNBS-subjected rats compared to control rats ($p < 0.001$). After pretreatment with compound **7b** or **13b** at a high dose, the fecal α1-AT levels were lessened compared to the TNBS group ($p < 0.01$, $p < 0.05$, respectively) and did not differ from those of control rats (p = NS in both cases). At a low dose, none of these two administered compounds had a significant effect on the fecal α1-AT concentration in comparison to the colitis group (p = NS). Similarly, compound **10b** (10 or 20 mg/kg) did not exert a significant effect on TNBS-caused alterations (p = NS in both cases).

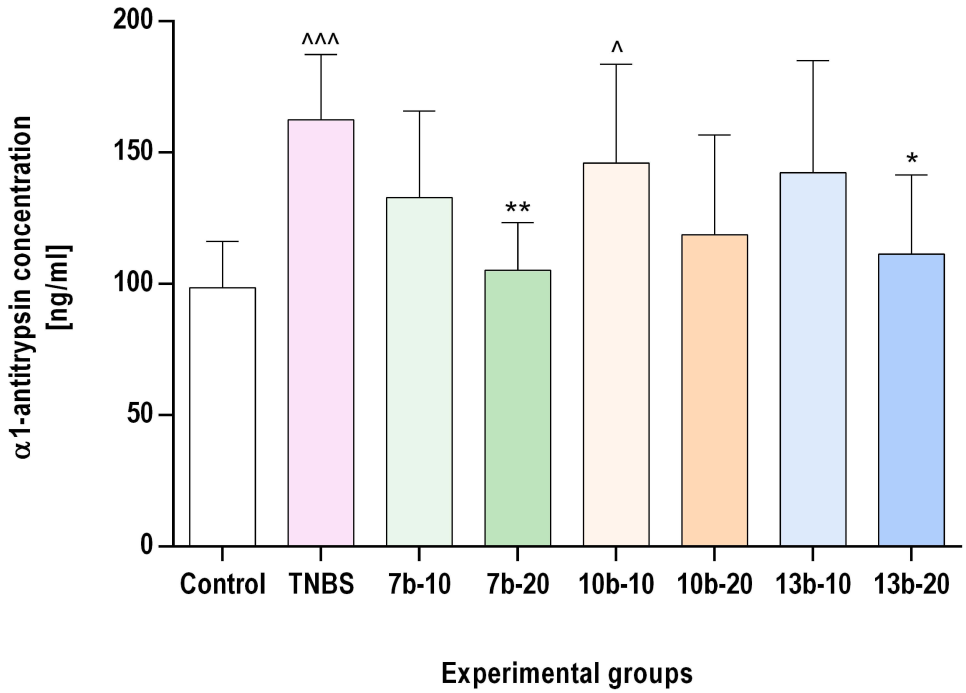

Figure 5 The influence of compounds **7b, 10b**, and **13b** on α1-AT concentration in feces samples. Experimental groups: control – control group; TNBS – group receiving only TNBS; **7b**-10, **7b**-20 – groups receiving, respectively, 10 or 20 mg/kg of studied compound **7b** and TNBS; **10b**-10, **10b**-20 – groups receiving, respectively, 10 or 20 mg/kg of studied compound **10b** and TNBS; **13b**-10, **13b**-20 – groups receiving, respectively, 10 or 20 mg/kg of studied compound **13b** and TNBS. Data are expressed as mean values ± SD; n = 10 for each group. Analyses were performed using the one-way ANOVA and Tukey's post hoc test. Differences $^{\wedge}p < 0.05$, $^{\wedge\wedge\wedge}p < 0.001$ vs control group; $^{*}p < 0.05$, $^{**}p < 0.01$ vs TNBS group were deemed statistically significant.

Pyrrolo[3,4-*d*]pyridazinone Derivatives Regulated the Colonic Levels of ERK1/2, JNK, and p38 in Rats with TNBS-Induced Colitis

To elucidate the mechanism of the protective effect of the studied compounds, the impact of new compounds on the MAPK signaling pathway was examined. As shown in Table 1, both total and phosphorylated MAPK protein (ERK1/2, JNK, p38) levels increased significantly following TNBS administration compared with control rats ($p < 0.05$, $p < 0.01$, $p < 0.01$ for total proteins and $p < 0.01$ $p < 0.01$, $p < 0.001$ for phosphoproteins, respectively). Pretreatment with compound **7b** at a high dose did not affect total ERK1/2, JNK, and p38 levels (p = NS in all cases). Contrary, compound **7b** at a high dose ameliorated the TNBS-induced elevation of the level of phosphorylated ERK1/2, JNK, and p38 ($p < 0.001$ vs TNBS group in all cases), yielding lower phosphorylated/total ratios than in the colitis group ($p < 0.05$ in all comparisons). The levels of phosphorylated ERK1/2 and JNK did not differ from those in the control group (p = NS), and the p38 phosphorylated level remained elevated compared to the control group ($p < 0.01$). Pretreatment with compound **13b** at a high dose did not affect total ERK1/2, JNK, and p38 levels (p = NS in all cases), while it counteracted the increase of phosphorylated p38 level ($p < 0.01$ vs TNBS), yielding a lessened p-p38/p38 ratio compared to the colitis group ($p < 0.05$). After pretreatment with a high dose of compound **13b**, the level of phosphorylated p38 remained, however, elevated compared to the control group ($p < 0.001$). In turn, compound **10b** administered at a high dose counteracted the TNBS-induced increase in total ERK1/2 and JNK levels ($p < 0.05$ vs TNBS and p = NS vs control group in both cases). No significant effect of studied compounds at a dose of 10 mg/kg on the level of total or phosphorylated ERK1/2, JNK, and p38 was observed (p = NS). Additionally, compound **7b** at a high dose lessened the p-JNK/JNK and p-p38/p38 ratio more effectively than compound **10b** at the corresponding dose ($p < 0.001$ and $p < 0.05$, respectively). Similarly, compound **13b** at a high dose lessened the p-JNK/JNK and p-p38/p38 ratio more effectively than compound **10b** at the corresponding dose ($p < 0.05$ in both comparisons). Compound **7b** at a high dose exerted a greater effect on the p-p38 level than at a low dose ($p < 0.05$).

https://doi.org/10.2147/JIR.S527041

Table 1 The Impact of Compounds **7b**, **10b**, and **13b** on Total and Phosphorylated ERK1/2, JNK, and p38 Expression in the Colon Tissues

Group	Parameter	Total [MFI/μg Protein]	Phosphorylated [MFI/μg Protein]	Phosphorylated/Total Ratio
Control	**ERK1/2**	1475.0±353.0	218.0±90.61	0.1434±0.0354
TNBS		1988.0±202.1$^{\wedge}$	371.5±85.10$^{\wedge\wedge}$	0.1921±0.0615
7b-10		1867.0±200.4	293.8±50.08	0.1582±0.0282
7b-20		1755.0±423.8	204.7±49.60***	0.1203±0.0294*
10b-10		1704.0±380.1	318.8±103.90	0.1955±0.0771
10b-20		1541.0±305.6*	290.0±81.02	0.1906±0.0511
13b-10		1866.0±314.8	333.3±97.20$^{\wedge}$	0.1855±0.0678
13b-20		1694.0±265.4	259.7±69.54	0.1519±0.0307
Control	**JNK**	60.78±19.03	12.93±6.04	0.2170±0.0632
TNBS		132.70±64.30$^{\wedge\wedge}$	29.62±13.42$^{\wedge\wedge}$	0.2248±0.0476
7b-10		116.80±28.47	22.13±8.11	0.1900±0.0482$^{\#\#}$
7b-20		92.11±54.59	9.15±6.05***	0.1046±0.0467$^{\wedge}$,*,$^{\#\#\#}$
10b-10		96.06±49.24	29.24±13.07$^{\wedge\wedge}$	0.3262±0.1093$^{\wedge}$
10b-20		68.77±33.02*	17.85±7.48	0.2981±0.1308
13b-10		106.70±39.29	20.89±10.72	0.1895±0.0356$^{\#\#}$
13b-20		94.28±34.92	16.56±6.66	0.1852±0.0693$^{\#}$
Control	**p38**	987.5±332.2	272.1±108.0	0.2873±0.1335
TNBS		1534.0±386.4$^{\wedge\wedge}$	1147.0±214.3$^{\wedge\wedge\wedge}$	0.7763±0.1574$^{\wedge\wedge\wedge}$
7b-10		1321.0±190.5	975.5±223.0$^{\wedge\wedge\wedge}$	0.7496±0.1941$^{\wedge\wedge\wedge}$
7b-20		1159.0±246.7	635.6±174.6$^{\wedge\wedge}$,***,$^{\&}$	0.5651±0.1720$^{\wedge\wedge}$,*,$^{\#}$
10b-10		1477.0±349.9$^{\wedge}$	1069.0±259.1$^{\wedge\wedge\wedge}$	0.7260±0.0843$^{\wedge\wedge\wedge}$
10b-20		1099.0±201.8	845.9±186.3$^{\wedge\wedge\wedge}$	0.7745±0.1377$^{\wedge\wedge\wedge}$
13b-10		1330.0±469.0	1109.0±343.3$^{\wedge\wedge\wedge}$	0.8496±0.1196$^{\wedge\wedge\wedge}$
13b-20		1321.0±329.5	730.3±169.9$^{\wedge\wedge\wedge}$,**	0.5665±0.1503$^{\wedge\wedge}$,*,$^{\#}$

Notes: Experimental groups: control – control group; TNBS – group receiving only TNBS; **7b**-10, **7b**-20 – groups receiving, respectively, 10 or 20 mg/kg of studied compound **7b** and TNBS; **10b**-10, **10b**-20 – groups receiving, respectively, 10 or 20 mg/kg of studied compound **10b** and TNBS; **13b**-10, **13b**-20 – groups receiving, respectively, 10 or 20 mg/kg of studied compound **13b** and TNBS. Data are expressed as mean values ± SD; n = 10 for each group. Analyses were performed using the one-way ANOVA and Tukey's post hoc test. Differences $^{\wedge}p < 0.05$, $^{\wedge\wedge}p < 0.01$, $^{\wedge\wedge\wedge}p < 0.001$ vs control group; $^{*}p < 0.05$, $^{**}p < 0.01$, $^{***}p < 0.001$ vs TNBS group; $^{\#}p < 0.05$, $^{\#\#}p < 0.01$, $^{\#\#\#}p < 0.001$ vs compound **10b** at the corresponding dose group; $^{\&}p < 0.05$ vs compound **7b**-10 group were deemed statistically significant.

Abbreviations: MFI, median fluorescence intensity; ERK1/2, extracellular signal-regulated kinase-1/2; JNK, c-Jun N-terminal kinase; p38, p38 kinase.

Multi-Criteria Decision Analysis (MCDA)

The results from each assay (histopathological assessment, immunohistochemical evaluation, multiplex, and ELISA assays) performed for studied pyrrolo[3,4-*d*]pyridazinone derivatives were examined by the MCDA to compare the effects of these new compounds on the intestinal barrier integrity. Based on the MCDA results (Figure 6), all tested compounds acted in a dose-dependent manner and the greatest protective effect on intestinal barrier integrity was found for compound **7b** at a dose of 20 mg/kg, followed by high-dose compound**13b**. Similar to our previous findings,[13] at both doses tested, compounds **7b** and **13b** were more effective than compound **10b**, and compound **7b** was more effective than compound **13b**.

Discussion

Crohn's disease and ulcerative colitis are the two main entities of IBD that primarily affect the gastrointestinal tract. The etiopathogenesis of IBD remains not entirely understood, which makes it one of the most challenging gastrointestinal diseases.[18] In the pathogenesis of IBD, an aberrant immune response triggered by the luminal antigen leads to mucosal inflammation that progressively disrupts the intestinal barrier. Compromised intestinal barrier integrity allows penetration

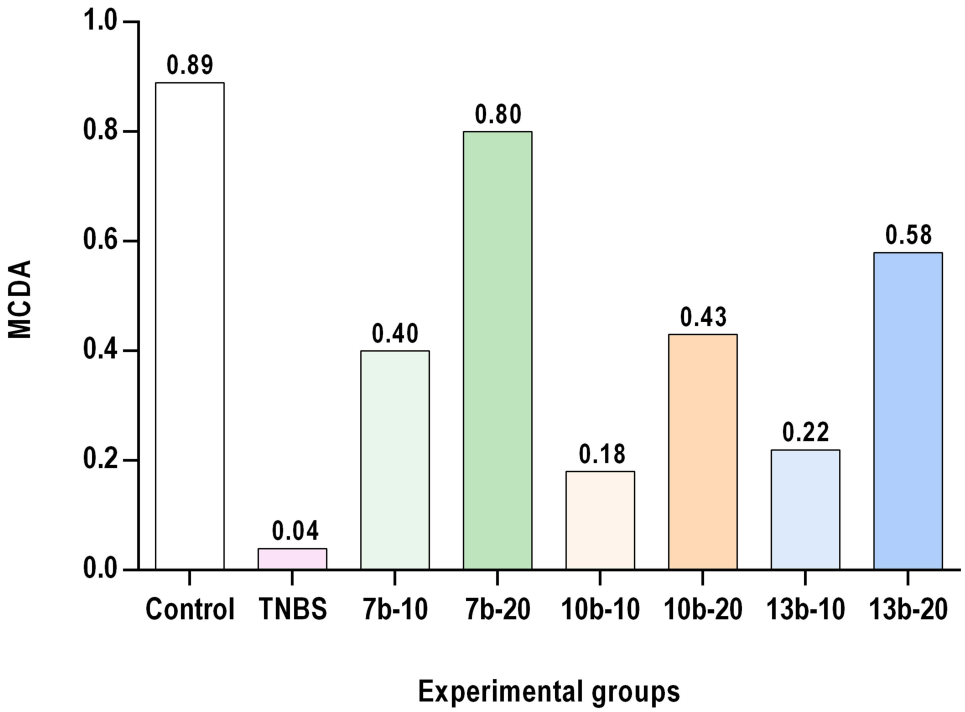

Figure 6 Multi-criteria decision analysis (MCDA) comparing the effect of the studied compounds **7b, 10b**, and **13b** on the integrity of the intestinal barrier by summarizing the results obtained in all bioassays performed.

of luminal antigens through the epithelium and reaches the underlying lamina propria causing overactivation of the mucosal immune system and further inflammation. Even though it remains not clear whether the intestinal barrier impairment precedes disease or results from mucosal inflammation, it constitutes a typical feature of IBD, suggesting that disruption of intestinal barrier integrity may predispose to the onset or worsening of IBD.[19] With the above in mind, targeting molecules associated with intestinal barrier disruption holds promise for the treatment and prevention of IBD.[1,5] The more so that in clinical studies, a sustained increase in intestinal permeability was a predictor of early relapse and poor prognosis in IBD patients, while the normalization of intestinal permeability after pharmacotherapy was a predictor of long-term remission.[20] Some findings have shown that a defect in the intestinal barrier alone is sufficient to elicit IBD.[2]

Intestinal barrier function is determined by interactions among several barrier components, especially epithelial tight junctions and a mucus layer. Impairment of the intestinal barrier characterized by the decreased expression of tight junction and mucus layer components is observed both in the pathogenesis of IBD and experimental colitis.[1,21,22]

In the colon, goblet cells are responsible for mucin secretion, and therefore their depletion in colitis may be at least partially responsible for the observed impairment of the epithelial barrier. In the reported study, we observed TNBS-induced irregular structure of goblet cells and a notable decrease in their mucous content. Pretreatment with compounds **7b** at both doses and **13b** at a high dose reversed this unfavorable trend and restored the crypt architecture and mucous secretion by goblet cells. Physiologically, goblet cells are filled up with mucin granules containing, among others, Muc2 and TFF3.[23,24] Muc2 polymers are densely packed in secretory vesicles of goblet cells, and upon secretion, they expand into a large net that covers and protects the epithelial surface.[23] TFF3 regulates mucus viscosity and epithelial regeneration, helping in this way to maintain mucosal barrier integrity.[24] Belle et al reported that the interplay between TFF3, LINGO2 (leucine-rich repeat and immunoglobulin-like domain-containing nogo receptor-interacting protein 2), and EGFR (epithelial growth factor receptor) may reduce the susceptibility to colitis.[24] It is suggested that damage of the mucosal barrier leads to dysregulation of mucosal immunity that is at least partially responsible for the loss of mucosal homeostasis and damage of the epithelial layer in IBD. Alternation of mucin secretion by goblet cells may weaken the physical barrier between luminal antigens and effector immune cells.[25] In our study, compounds **7b** and **13b** in high

https://doi.org/10.2147/JIR.S527041

doses (20 mg/kg) increased Muc2 and TFF3 expression in goblet cells. Our findings suggest that both compounds may exert a favorable effect on the mucus layer that protects intestinal epithelial and immune cells against luminal antigens.

Apart from the mucus layer, the epithelial tight junctions are the cornerstones of the mechanism that preserves intestinal integrity. Epithelial tight junctions are composed of transmembrane and cytosolic proteins, including among others claudins (CLDN) and occludin (OCLN) that interact with cytoplasmic proteins such as zonula occludens (ZO) and junctional adhesion molecules (JAM).[5,6] Although it is confirmed that tight junctions are crucial for the maintenance of intestinal barrier integrity, the exact function of the individual proteins remains not fully explained.[26] In our study in the TNBS group, we observed decreased levels of CLDN1, OCLN, and ZO1 in the colon tissue that was accompanied by an increased fecal concentration of α1-AT. These findings support the hypothesis about the important role of tight junction proteins in the maintenance of the integrity of the epithelial barrier. Decreased expression of tight junction proteins associated with increased epithelial permeability in experimental colitis was also reported by other authors.[27–30] In the reported study, compounds **7b** and **13b** in high doses (20 mg/kg) increased the expression of tight junction proteins (CLDN1, OCLN, ZO1) simultaneously reducing the fecal concentration of α1-AT. These findings, in combination with their influence on goblet cell architecture and secretory function reported above, support the hypothesis about their beneficial effect on epithelial barrier integrity and permeability. Pretreatment with compound **10b** increased the expression of CLDN1 and OCLN, however, it did not alleviate TNBS-induced suppression of ZO1. Although it counteracted the TNBS-induced down-regulation of CLDN1 and OCLN synthesis, it did not restore crypt architecture, nor Muc2 and TFF3 secretion. These findings suggest that ZO1 plays a crucial role in epithelial barrier integrity. Our results are consistent with Kuo et al,[31] whose findings show that ZO1 is critical to mucosal repair, and the loss of ZO1 in both human and experimental IBD may be one reason for ineffective mucosal healing and promote disease progression. Given that in our previous study,[13] compounds **7b** and **13b**, but not **10b**, alleviated symptoms of experimental colitis, it can be assumed that normalizing the ZO1 as well as restored Muc2, TFF3 expression, and goblet cell function by compounds **7b** and **13b** corresponds to enhancing mucosal healing and promoting the resolution of active disease.

The MAPK signaling pathway has been shown to be essential in disrupting the intestinal barrier.[32] There is increasing evidence from in vitro and in vivo studies that excessive activation of ERK1/2,[33,34] JNK,[9,35] and p38[9,36,37] contributes to impaired integrity of the tight junctions and the mucus layer and, thus, to increased intestinal permeability. Although the role of MAPK activation in IBD and other inflammatory conditions is not entirely clear, increased phosphorylation of ERK1/2, JNK, and p38 is observed both in the inflamed colonic epithelium of IBD patients and experimental colitis.[35,38–41] For these reasons, pharmacological inhibition of ERK1/2, JNK, or p38 activation may afford therapeutic benefits in diseases associated with impaired epithelial barrier function, including inflammatory bowel disease. This kind of action has been demonstrated in this study.

One mechanism by which ERK1/2, JNK, and p38 overactivation causes TJ disruption is the downregulation of claudin-1, occludin, and ZO1.[28,32,33,42] In the present study, pretreatment with compound **7b** at a high dose protected against TNBS-induced activation of all studied MAP kinases as evidenced by the decrease of p-ERK1/2, p-JNK, and p-p38 levels and the ratios of phosphorylated to total ERK1/2, JNK, and p38, whereas pretreatment with compound **13b** at a high dose prevented TNBS-induced phosphorylation of p38 kinase only as evidenced by p-p38 level and the ratio of phosphorylated to total p38. This suggests that compound **7b** could elevate the levels of tight junction components (CLDN1, OCLN, ZO1) and mucus layer proteins (Muc2, TFF3) and enhance intestinal barrier integrity through the inhibition of ERK1/2, JNK, and p38 phosphorylation. This is consistent with our previous results that compound **7b** and **13b**, but not compound **10b**, alleviated symptoms of experimental colitis.[13] Considering that compound **13b** inhibits p38 phosphorylation only, and its effect on the levels of tight junction proteins and α1-antitrypsin is not less than that of compound **7b**, it may be concluded that the inhibition of p38 is crucial to prevent TJ integrity. This is consistent with Carrozzino's findings[9] that blocking p38 or JNK signaling is sufficient to enhance epithelial barrier function and that simultaneous inhibition of both the p38 and JNK pathways has only a slight additional effect compared to the inhibition of a single pathway. Interestingly, according to previous studies, the effect of ERK1/2 on intestinal barrier function is controversial.[33] Some studies have shown to enhance intestinal epithelial barrier function by downregulating ERK1/2,[43] while others have been shown to improve the intestinal epithelial barrier by upregulating the ERK1/2 pathway.[44] This discrepancy may result from the fact that the ERK1/2 effect on the intestinal barrier is ligand-dependent.[9] When activation of ERK1/2 is induced by IL-17 (such as in human IBD[45,46] or

TNBS-evoked experimental colitis[13,47]) it results in decreased tight junction protein expression and impaired tight junction barrier function in intestinal epithelial cells.[9]

It has been also reported that activated ERK1/2 and JNK can inhibit the expression of Muc2, thereby causing a loss of the protective mucus layer and damage to the underlying epithelium.[48–51] In the present study, compound **7b** ameliorated the TNBS-induced overexpression of phosphorylated ERK1/2, JNK, and p38, whereas compound **13b** reduced only phosphorylation of p38, leading simultaneously to the increase in the expression Muc2. These observations suggest that the beneficial influence of the investigated compounds **7b** and **13b** on the secretory function of goblet cells and mucin secretion may be mediated through the inhibition of phosphorylation of MAPK proteins. Warmus et al[52] reported that some other 1,3,4-oxadiazole derivatives acted as ERK1/2 inhibitors, causing a decrease in p-ERK levels in mice. The phosphorylation of ERK1/2[53] and p38[54–56] was also inhibited by other compounds based on the pyridazinone scaffold in computational and in vitro studies.

Overactivity of MMP9, matrix metalloproteinase classified as gelatinase, has been identified as the factor that may increase intestinal permeability in the p38 kinase-dependent manner.[57] MMP9 has proinflammatory properties and its up-regulation has been demonstrated in patients with IBD and experimental colitis.[58,59] It was also reported that its fecal and serum concentration correlate with IBD activity.[59] Research on the intracellular mechanism of MMP9-induced disruption of the intestinal tight junction barrier concluded that MMP9 activates MAPK, including ERK1/2, JNK, p38, and myosin light chain kinase (MLCK), leading to increased intestinal permeability.[60] Additionally, it has been reported that overexpression of MMP9 inhibits the differentiation of goblet cells and thus decreases Muc2 secretion, leading to the dysfunction of the mucous barrier.[10] In our study, compounds **7b** at both doses and **13b** at a high dose, significantly reduced TNBS-induced MMP9 synthesis. This observation at least partially explains their beneficial influence on the intestinal barrier. Other authors reported that both 1,3,4-oxadiazole and pyridazinone-scaffold-based molecules decrease the expression of MMP9 in computational and in vitro studies,[61–63] which is in line with our observations.

To the best of our knowledge, our study is the first to evaluate the effect of 1,3,4-oxadiazole derivatives of pyrrolo [3,4-*d*]pyridazinone on the intestinal barrier in experimental colitis. Although our in vivo findings demonstrated a beneficial effect of the tested 1,3,4-oxadiazole derivatives of pyrrolo[3,4-*d*]pyridazinone on restoring the integrity of the mucosal epithelial barrier, further investigation into the underlying molecular mechanisms is warranted. For instance, Caco-2 cell layer permeability assays and mucus secretion function tests may offer deeper insights into how these compounds modulate barrier function at the cellular level.

It may be concluded that the protective activity of compounds **7b** and **13b** is due to their enhancement effect on intestinal barrier function reflected by increased tight junction and mucus layer integrity (Figure 7). Our findings provide novel insights into the mechanisms of the studied compounds for potential uses in intestinal barrier loss-dependent conditions, including IBD.

Conclusion

Collectively, the findings provided herein support the conclusion that two of the studied new pyrrolo[3,4-*d*]pyridazinone derivatives, ie, 6-butyl-3,5,7-trimethyl-1-[[3-[(4-phenylpiperazin-1-yl)methyl]-2-thioxo-1,3,4-oxadiazol-5-yl]methoxy] pyrrolo[3,4-*d*]pyridazin-4-one and 6-butyl-1-[[3-[[4-(4-chlorophenyl)-4-hydroxy-1-piperidyl]methyl]-2-thioxo-1,3,4-oxadiazol-5-yl]methoxy]-3,5,7-trimethyl-pyrrolo[3,4-*d*]pyridazin-4-one, called the compounds **7b** and **13b**, respectively, contribute to the restoration of the intestinal barrier and improve epithelial integrity in the preclinical model of IBD. In rats with experimental colitis, both these compounds at a dose of 20 mg/kg reestablished colonic levels of tight junction (claudin 1, occludin, zonula occludens 1) and mucus-related proteins (mucin 2, trefoil factor 3) and prevented goblet cell depletion and mucus layer disruption. Both these compounds also normalized the level of the functional parameter, fecal α1-antitrypsin. Furthermore, they mitigated the TNBS-induced elevation of MMP9 levels and activation of MAPKs. The restoration of the intestinal barrier is of key importance in the management of inflammatory bowel disease because it can modulate and even reverse the self-perpetuating inflammatory process by limiting the interaction between the internal milieu and the gut lumen.

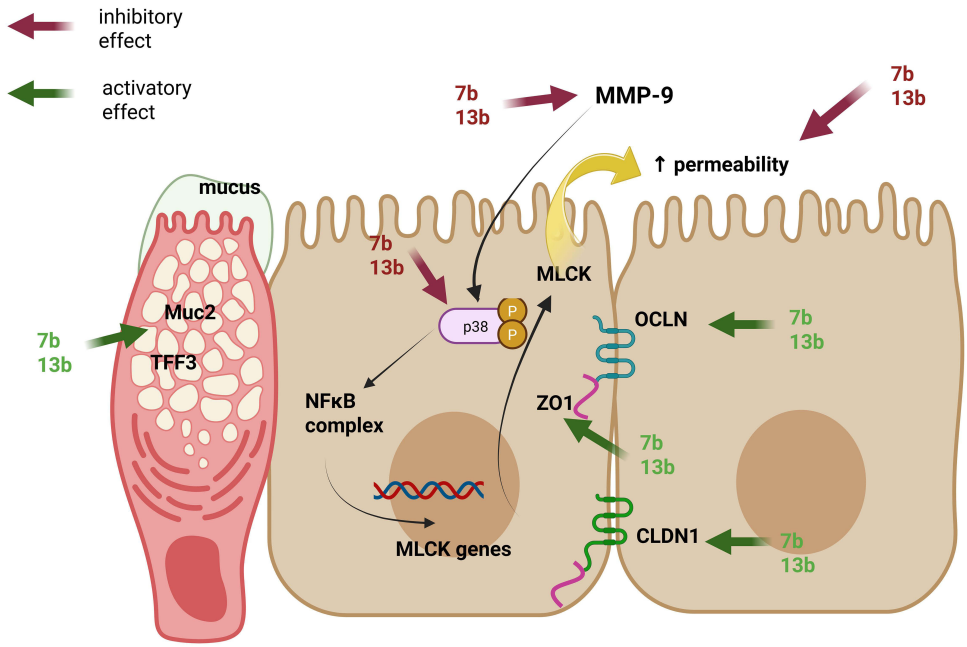

Figure 7 The influence of compounds **7b** and **13b** on intestinal epithelial barrier. Both compounds increase (green arrows) the expression of thigh junction proteins (CLDN1 – claudin 1, OCLN – occludin, ZO1 – zonula occludens 1) in intestinal epithelial cells, as well as mucin 2 (Muc2) and trefoil factor 3 (TFF3) in goblet cells. They inhibit (red arrows) the activity of proinflammatory matrix metalloproteinase-9 (MMP-9) and decrease the phosphorylation of p38 kinase. Compound **7b** additionally inhibits the phosphorylation of other mitogen-activated protein kinases (MAPK): extracellular signal-regulated kinase-1/2 (ERK1/2) and c-Jun N-terminal kinase (JNK). As a consequence, they decrease the permeability of the intestinal epithelial barrier. (Created with BioRender.com).

Data Sharing Statement

The data underlying this article will be shared upon request to the corresponding author.

Ethics Statement

The experimental protocol was approved (Resolution No. 005/2020 of 15 January 2020) by the Local Ethics Committee for Animal Experiments in Wrocław at Hirszfeld Institute of Immunology and Experimental Therapy of the Polish Academy of Sciences (Wrocław, Poland). The welfare of laboratory animals and all experimental procedures complied with international, national, and institutional guidelines, including the Act of 15 January 2015 on the protection of animals used for scientific and educational purposes (Journal of Laws of 2015, item 266), the EU directive 2010/63/EU, and National Institutes of Health Guide for the Care and Use of Laboratory Animals.

Acknowledgments

The authors would like to thank Alicja Tomaszek, Aneta Cieśla-Niechwiadowicz, Joanna Kwiatkowska, and Paulina Jawień for technical assistance in conducting the experiments and Kamila Czyszczoń and Maja Lipińska for support with animal maintenance and care.

Author Contributions

All authors made a significant contribution to the work reported, whether that is in the conception, study design, execution, acqui-sition of data, analysis and interpretation, or in all these areas; took part in drafting, revising or critically reviewing the article; gave final approval of the version to be published; have agreed on the journal to which the article has been submitted; and agree to be accountable for all aspects of the work.

Funding

This research benefited from a grant from the National Science Centre of Poland (Grant No. 2019/03/X/NZ7/0180) and Wroclaw Medical University (Grant No. SUBZ.A080.22.076).

Disclosure

The authors report no conflicts of interest in this work.

References

1. Bischoff SC, Barbara G, Buurman W, et al. Intestinal permeability--a new target for disease prevention and therapy. *BMC Gastroenterol*. 2014;14:189. doi:10.1186/s12876-014-0189-7
2. Martini E, Krug SM, Siegmund B, Neurath MF, Becker C. Mend your fences: the epithelial barrier and its relationship with mucosal immunity in inflammatory bowel disease. *Cell Mol Gastroenterol Hepatol*. 2017;4(1):33–46. doi:10.1016/j.jcmgh.2017.03.007
3. Martens EC, Neumann M, Desai MS. Interactions of commensal and pathogenic microorganisms with the intestinal mucosal barrier. *Nat Rev Microbiol*. 2018;16(8):457–470. doi:10.1038/s41579-018-0036-x
4. Pelaseyed T, Bergström JH, Gustafsson JK, et al. The mucus and mucins of the goblet cells and enterocytes provide the first defense line of the gastrointestinal tract and interact with the immune system. *Immunol Rev*. 2014;260(1):8–20. doi:10.1111/imr.12182
5. Odenwald MA, Turner JR. The intestinal epithelial barrier: a therapeutic target? *Nat Rev Gastroenterol Hepatol*. 2017;14(1):9–21. doi:10.1038/nrgastro.2016.169
6. Panwar S, Sharma S, Tripathi P. Role of barrier integrity and dysfunctions in maintaining the healthy gut and their health outcomes. *Front Physiol*. 2021;12:715611. doi:10.3389/fphys.2021.715611
7. Peterson LW, Artis D. Intestinal epithelial cells: regulators of barrier function and immune homeostasis. *Nat Rev Immunol*. 2014;14(3):141–153. doi:10.1038/nri3608
8. Capaldo CT, Powell DN, Kalman D. Layered defense: how mucus and tight junctions seal the intestinal barrier. *J Mol Med*. 2017;95(9):927–934. doi:10.1007/s00109-017-1557-x
9. Carrozzino F, Pugnale P, Féraille E, Montesano R. Inhibition of basal p38 or JNK activity enhances epithelial barrier function through differential modulation of claudin expression. *Am J Physiol Cell Physiol*. 2009;297(3):C775–787. doi:10.1152/ajpcell.00084.2009
10. O'Sullivan S, Gilmer JF, Medina C. Matrix metalloproteinases in inflammatory bowel disease: an update. *Mediators Inflamm*. 2015;2015:964131. doi:10.1155/2015/964131
11. Bernardi S, Del Bo' C, Marino M, et al. Polyphenols and intestinal permeability: rationale and future perspectives. *J Agric Food Chem*. 2020;68(7):1816–1829. doi:10.1021/acs.jafc.9b02283
12. Szandruk-Bender M, Merwid-Ląd A, Wiatrak B, et al. Novel 1,3,4-oxadiazole derivatives of Pyrrolo[3,4-*d*]Pyridazinone exert anti-inflammatory activity without acute gastrotoxicity in the carrageenan-induced rat paw edema test. *JIR*. 2021;14:5739–5756. doi:10.2147/JIR.S330614
13. Szandruk-Bender M, Wiatrak B, Dzimira S, et al. Targeting lineage-specific transcription factors and cytokines of the Th17/Treg axis by novel 1,3,4-oxadiazole derivatives of pyrrolo[3,4-*d*]pyridazinone attenuates TNBS-induced experimental colitis. *Int J Mol Sci*. 2022;23(17):9897. doi:10.3390/ijms23179897
14. Szczukowski Ł, Redzicka A, Wiatrak B, et al. Design, synthesis, biological evaluation and in silico studies of novel pyrrolo[3,4-*d*]pyridazinone derivatives with promising anti-inflammatory and antioxidant activity. *Bioorg Chem*. 2020;102:104035. doi:10.1016/j.bioorg.2020.104035
15. Szandruk-Bender M, Wiatrak B, Szczukowski Ł, et al. Novel 1,3,4-oxadiazole derivatives of Pyrrolo[3,4-*d*]pyridazinone exert antinociceptive activity in the tail-flick and formalin test in rodents and reveal reduced gastrotoxicity. *Int J Mol Sci*. 2020;21(24):9685. doi:10.3390/ijms21249685
16. Morris GP, Beck PL, Herridge MS, Depew WT, Szewczuk MR, Wallace JL. Hapten-induced model of chronic inflammation and ulceration in the rat colon. *Gastroenterology*. 1989;96(3):795–803.
17. Zhang C, Monk JM, Lu JT, et al. Cooked navy and black bean diets improve biomarkers of colon health and reduce inflammation during colitis. *Br J Nutr*. 2014;111(9):1549–1563. doi:10.1017/S0007114513004352
18. Gálvez J. Role of Th17 cells in the pathogenesis of human IBD. *ISRN Inflamm*. 2014;2014:e928461. doi:10.1155/2014/928461
19. Michielan A, D'Incà R. Intestinal permeability in inflammatory bowel disease: pathogenesis, clinical evaluation, and therapy of leaky gut. *Mediators Inflamm*. 2015;2015:628157. doi:10.1155/2015/628157
20. Al-Sadi R, Ye D, Boivin M, et al. Interleukin-6 modulation of intestinal epithelial tight junction permeability is mediated by JNK pathway activation of claudin-2 gene. *PLoS One*. 2014;9(3):e85345. doi:10.1371/journal.pone.0085345
21. Pastorelli L, De Salvo C, Mercado JR, Vecchi M, Pizarro TT. Central role of the gut epithelial barrier in the pathogenesis of chronic intestinal inflammation: lessons learned from animal models and human genetics. *Front Immunol*. 2013;4:280. doi:10.3389/fimmu.2013.00280
22. Lechuga S, Ivanov AI. Disruption of the epithelial barrier during intestinal inflammation: quest for new molecules and mechanisms. *Biochim Biophys Acta Mol Cell Res*. 2017;1864(7):1183–1194. doi:10.1016/j.bbamcr.2017.03.007
23. Birchenough GMH, Johansson MEV, Gustafsson JK, Bergström JH, Hansson GC. New developments in goblet cell mucus secretion and function. *Mucosal Immunol*. 2015;8(4):712–719. doi:10.1038/mi.2015.32
24. Belle NM, Ji Y, Herbine K, et al. TFF3 interacts with LINGO2 to regulate EGFR activation for protection against colitis and gastrointestinal helminths. *Nat Commun*. 2019;10(1):4408. doi:10.1038/s41467-019-12315-1
25. Dharmani P, Strauss J, Ambrose C, Allen-Vercoe E, Chadee K. Fusobacterium nucleatum infection of colonic cells stimulates MUC2 mucin and tumor necrosis factor alpha. *Infect Immun*. 2011;79(7):2597–2607. doi:10.1128/IAI.05118-11
26. Chelakkot C, Ghim J, Ryu SH. Mechanisms regulating intestinal barrier integrity and its pathological implications. *Exp Mol Med*. 2018;50(8):1–9. doi:10.1038/s12276-018-0126-x
27. Sharma D, Malik A, Guy CS, Karki R, Vogel P, Kanneganti TD. Pyrin inflammasome regulates tight junction integrity to restrict colitis and tumorigenesis. *Gastroenterology*. 2018;154(4):948–964.e8. doi:10.1053/j.gastro.2017.11.276
28. Ran X, Li Y, Chen G, et al. Farrerol ameliorates TNBS-induced colonic inflammation by inhibiting ERK1/2, JNK1/2, and NF-κB signaling pathway. *Int J Mol Sci*. 2018;19(7):2037. doi:10.3390/ijms19072037
29. Wang J, Zhang C, Guo C, Li X. Chitosan ameliorates DSS-induced ulcerative colitis mice by enhancing intestinal barrier function and improving microflora. *Int J Mol Sci*. 2019;20(22):5751. doi:10.3390/ijms20225751
30. Zhang J, Lei H, Hu X, Dong W. Hesperetin ameliorates DSS-induced colitis by maintaining the epithelial barrier via blocking RIPK3/MLKL necroptosis signaling. *Eur J Pharmacol*. 2020;873:172992. doi:10.1016/j.ejphar.2020.172992

31. Kuo WT, Zuo L, Odenwald MA, et al. The tight junction protein ZO-1 is dispensable for barrier function but critical for effective mucosal repair. *Gastroenterology*. 2021;161(6):1924–1939. doi:10.1053/j.gastro.2021.08.047
32. Zhang Z, Zhang Q, Li F, Xin Y, Duan Z. Contributions of HO-1-dependent MAPK to regulating intestinal barrier disruption. *Biomol Ther*. 2021;29 (2):175–183. doi:10.4062/biomolther.2020.112
33. Zhai Z, Ni X, Jin C, et al. Cecropin A modulates tight junction-related protein expression and enhances the barrier function of porcine intestinal epithelial cells by suppressing the MEK/ERK pathway. *Int J Mol Sci*. 2018;19(7):1941. doi:10.3390/ijms19071941
34. Huang Y, Wang C, Tian X, et al. Pioglitazone attenuates experimental colitis-associated hyperalgesia through improving the intestinal barrier dysfunction. *Inflammation*. 2020;43(2):568–578. doi:10.1007/s10753-019-01138-3
35. Deng J, Zeng L, Lai X, et al. Metformin protects against intestinal barrier dysfunction via AMPKα1-dependent inhibition of JNK signalling activation. *J Cell Mol Med*. 2018;22(1):546–557. doi:10.1111/jcmm.13342
36. Li Y, Xu B, Xu M, et al. 6-Gingerol protects intestinal barrier from ischemia/reperfusion-induced damage via inhibition of p38 MAPK to NF-κB signalling. *Pharmacol Res*. 2017;119:137–148. doi:10.1016/j.phrs.2017.01.026
37. Li C, Bai X, Liu X, et al. Disruption of epithelial barrier of Caco-2 cell monolayers by excretory secretory products of trichinella spiralis might be related to serine protease. *Front Microbiol*. 2021;12:634185. doi:10.3389/fmicb.2021.634185
38. Waetzig GH, Seegert D, Rosenstiel P, Nikolaus S, Schreiber S. p38 mitogen-activated protein kinase is activated and linked to TNF-α signaling in inflammatory bowel disease. *J Immunol*. 2002;168(10):5342–5351. doi:10.4049/jimmunol.168.10.5342
39. Roy PK, Rashid F, Bragg J, Ibdah JA. Role of the JNK signal transduction pathway in inflammatory bowel disease. *World J Gastroenterol*. 2008;14 (2):200–202. doi:10.3748/wjg.14.200
40. Yang XL, Guo TK, Wang YH, et al. Ginsenoside Rd attenuates the inflammatory response via modulating p38 and JNK signaling pathways in rats with TNBS-induced relapsing colitis. *Int Immunopharmacol*. 2012;12(2):408–414. doi:10.1016/j.intimp.2011.12.014
41. Samak G, Chaudhry KK, Gangwar R, Narayanan D, Jaggar JH, Rao R. Calcium/Ask1/MKK7/JNK2/c-Src signalling cascade mediates disruption of intestinal epithelial tight junctions by dextran sulfate sodium. *Biochem J*. 2015;465(3):503–515. doi:10.1042/BJ20140450
42. Sun L, Xu C, Chen G, et al. A novel role of OS-9 in the maintenance of intestinal barrier function from hypoxia-induced injury via p38-dependent pathway. *Int J Biol Sci*. 2015;11(6):664–671. doi:10.7150/ijbs.10783
43. Piegholdt S, Pallauf K, Esatbeyoglu T, et al. Biochanin A and prunetin improve epithelial barrier function in intestinal CaCo-2 cells via downregulation of ERK, NF-κB, and tyrosine phosphorylation. *Free Radic Biol Med*. 2014;70:255–264. doi:10.1016/j.freeradbiomed.2014.02.025
44. Wang K, Jin X, Chen Y, et al. Polyphenol-rich propolis extracts strengthen intestinal barrier function by activating AMPK and ERK signaling. *Nutrients*. 2016;8(5):272. doi:10.3390/nu8050272
45. Patel DD, Kuchroo VK. Th17 cell pathway in human immunity: lessons from genetics and therapeutic interventions. *Immunity*. 2015;43 (6):1040–1051. doi:10.1016/j.immuni.2015.12.003
46. Yan JB, Luo MM, Chen ZY, He BH. The function and role of the Th17/Treg cell balance in inflammatory bowel disease. *J Immunol Res*. 2020;2020:8813558. doi:10.1155/2020/8813558
47. Szandruk-Bender M, Rutkowska M, Merwid-Ląd A, et al. Cornelian cherry iridoid-polyphenolic extract improves mucosal epithelial barrier integrity in rat experimental colitis and exerts antimicrobial and antiadhesive activities in vitro. *Oxid Med Cell Longev*. 2020;2020:7697851. doi:10.1155/2020/7697851
48. Ahn DH, Crawley SC, Hokari R, et al. TNF-alpha activates MUC2 transcription via NF-kappaB but inhibits via JNK activation. *Cell Physiol Biochem*. 2005;15(1–4):29–40. doi:10.1159/000083636
49. Hokari R, Lee H, Crawley SC, et al. Vasoactive intestinal peptide upregulates MUC2 intestinal mucin via CREB/ATF1. *Am J Physiol Gastrointest Liver Physiol*. 2005;289(5):G949–959. doi:10.1152/ajpgi.00142.2005
50. Lemieux E, Boucher MJ, Mongrain S, Boudreau F, Asselin C, Rivard N. Constitutive activation of the MEK/ERK pathway inhibits intestinal epithelial cell differentiation. *Am J Physiol Gastrointest Liver Physiol*. 2011;301(4):G719–730. doi:10.1152/ajpgi.00508.2010
51. Wang R, Kwon IK, Singh N, et al. Type 2 cGMP-dependent protein kinase regulates homeostasis by blocking c-Jun N-terminal kinase in the colon epithelium. *Cell Death Differ*. 2014;21(3):427–437. doi:10.1038/cdd.2013.163
52. Warmus JS, Flamme C, Zhang LY, et al. 2-Alkylamino- and alkoxy-substituted 2-amino-1,3,4-oxadiazoles—O-Alkyl benzohydroxamate esters replacements retain the desired inhibition and selectivity against MEK (MAP ERK kinase). *Bioorg Med Chem Lett*. 2008;18(23):6171–6174. doi:10.1016/j.bmcl.2008.10.015
53. Wang Y, Dai Y, Wu X, et al. Discovery and development of a series of Pyrazolo[3,4-d]pyridazinone compounds as the novel covalent fibroblast growth factor receptor inhibitors by the rational drug design. *J Med Chem*. 2019;62(16):7473–7488. doi:10.1021/acs.jmedchem.9b00510
54. Tynebor RM, Chen MH, Natarajan SR, et al. Synthesis and biological activity of pyridopyridazin-6-one p38 MAP kinase inhibitors. Part 1. *Bioorg Med Chem Lett*. 2011;21(1):411–416. doi:10.1016/j.bmcl.2010.10.128
55. Singh J, Sharma D, Bansal R. Pyridazinone: an attractive lead for anti-inflammatory and analgesic drug discovery. *Future Med Chem*. 2017;9 (1):95–127. doi:10.4155/fmc-2016-0194
56. Tripathi DK, Poluri KM. Molecular insights into kinase mediated signaling pathways of chemokines and their cognate G protein coupled receptors. *FBL*. 2020;25(7):1361–1385. doi:10.2741/4860
57. Al-Sadi R, Engers J, Haque M, King S, Al-Omari D, Ma TY. Matrix Metalloproteinase-9 (MMP-9) induced disruption of intestinal epithelial tight junction barrier is mediated by NF-κB activation. *PLoS One*. 2021;16(4):e0249544. doi:10.1371/journal.pone.0249544
58. Heimesaat MM, Dunay IR, Fuchs D, et al. The distinct roles of MMP-2 and MMP-9 in acute DSS colitis. *Eur J Microbiol Immunol*. 2011;1 (4):302–310. doi:10.1556/EuJMI.1.2011.4.6
59. Jakubowska K, Pryczynicz A, Iwanowicz P, et al. Expressions of matrix metalloproteinases (MMP-2, MMP-7, and MMP-9) and their inhibitors (TIMP-1, TIMP-2) in inflammatory bowel diseases. *Gastroenterol Res Pract*. 2016;2016:2456179. doi:10.1155/2016/2456179
60. Al-Sadi R, Youssef M, Rawat M, et al. MMP-9-induced increase in intestinal epithelial tight permeability is mediated by p38 kinase signaling pathway activation of MLCK gene. *Am J Physiol Gastrointest Liver Physiol*. 2019;316(2):G278–G290. doi:10.1152/ajpgi.00126.2018
61. Özdemir A, Sever B, Altıntop MD, et al. Synthesis and evaluation of new oxadiazole, thiadiazole, and triazole derivatives as potential anticancer agents targeting MMP-9. *Molecules*. 2017;22(7):1109. doi:10.3390/molecules22071109

62. Rubina B. Recent developments on pharmacological potential of 1,3,4-oxadiazole scaffold. *Indian J Pharm Educ Res*. 2019;53(2s):s1–s16. doi:10.5530/ijper.53.2s.44
63. Moniot A, Braux J, Siboni R, et al. Inhibition of recruitment and activation of neutrophils by pyridazinone-scaffold-based compounds. *Int J Mol Sci*. 2022;23(13):7226. doi:10.3390/ijms23137226